SAGE−Spectroscopy: The life cycle of dust and gas in the Large Magellanic Cloud

Principal Investigator: Alexander G.G.M. Tielens (ES, ISM, SF)

Institution: NASA Ames Research Center

Electronic mail: atielens@mail.arc.nasa.gov

Technical Contact: Ciska Markwick−Kemper, University of Manchester (SC, ES, ISM)

Co−Investigators: Jean−Philippe Bernard, CESR, Toulouse (ISM, SF)

Robert Blum, NOAO (ES)

Martin Cohen , UC−Berkeley (ES, SC)

Catharinus Dijkstra, unaff. (ES)

Karl Gordon, U. Arizona (IRSE, MP, ME, ISM, SF)

Varoujan Gorjian, NASA−JPL (SC)

Jason Harris, U. Arizona (SC, ES)

Sacha Hony, CEA, Saclay (ISM, SF)

Joseph Hora, CfA−Harvard (ES)

Remy Indebetouw, U. Virginia (IRSE, SF)

Eric Lagadec, U. of Manchester (ES)

Jarron Leisenring, U. of Virginia (IRSP, ES)

Suzanne Madden, CEA,Saclay (ISM, SF)

Massimo Marengo, CfA−Harvard (SC)

Mikako Matsuura, NAO, Japan (ES)

Margaret Meixner, STScI (DB, ES, SC, SF)

Knut Olsen, NOAO (ES)

Roberta Paladini, IPAC/CalTech (SF)

Deborah Paradis, CESR, Toulouse (ISM)

William T. Reach, IPAC/CalTech (IRSE, ISM)

Douglas Rubin, CEA, Saclay (ISM, SF)

Marta Sewilo, STSci (DB, SF, SC)

Greg Sloan, Cornell (IRSP, SC, ES)

Angela Speck, U. Missouri (ES)
Sundar Srinivasan, Johns Hopkins U. (ES)
Schuyler Van Dyk, Spitzer Science Center (IRSP, SC)
Jacco van Loon, U. of Keele (MP, ES)
Uma Vijh, STSci and U. of Toledo (DB, ES, ISM)
Kevin Volk, Gemini Observatory (ES, SC)
Barbara Whitney, Space Science Institute (SF, SC)
Albert Zijlstra, U. of Manchester (ES)

Science Category: Extragalactic: local group galaxies

Observing Modes: IRS Staring, IRS Mapping, MIPS SED

Hours Requested: 224.4

Proprietary Period(days): 0

Abstract:
Cycling of matter between the ISM and stars drives the evolution of a galaxy's visible matter and its emission characteristics. To understand this recycling, the SAGE legacy project has surveyed the Large Magellanic Cloud with IRAC and MIPS to study the physical processes of the ISM, the formation of new stars and the injection of mass by evolved stars and their relationships on the galaxy−wide scale. Due to its proximity, favorable viewing angle, and multi−wavelength information, the LMC is uniquely suited to survey the agents of a galaxy's evolution, the ISM and stars.

We propose to leverage the SAGE legacy program to conduct a comprehensive IRS and MIPS−SED spectroscopy program of dust with the goal to determine the composition, origin, evolution, and observational characteristics of interstellar dust and its role in the LMC. Analysis of the spectra will yield composition and abundance of the dust compounds in different LMC objects, including AGB stars, post−AGB, young stellar objects, HII regions and the general diffuse ISM and provide a quantitative picture of the dust lifecyle. Besides dust features, the spectra will also contain molecular and atomic emission and absorption lines, providing the diagnostics to determine physical parameters such as temperature, density and radiation field − all important to the formation and processing of dust, and understanding the life cycle of matter.

The proposed spectroscopic survey will provide critical underpinning for the SAGE survey by linking observed IRAC and MIPS colors of LMC objects to the infrared spectral type of the object. We will to the maximum extent utilize the LMC spectroscopy available in the Spitzer archive. A subset of the IRS point sources from this proposal will also be surveyed in MIPS SED. Legacy data products that will be made available to the public include all reduced single point spectra and data cubes, feature maps, a spectral catalog, and a fully classified SAGE point source catalog.

1 Scientific Justification

1.1 The life cycle of dust in the Large Magellanic Cloud

The interstellar medium (ISM) plays a central role in the evolution of galaxies as the birthsite of new stars and the repository of old stellar ejecta. The formation of new stars slowly consumes the ISM, locking it up for millions to billions of years. As these stars age, the winds from low mass, asymptotic giant branch (AGB) stars and high mass, red supergiants (RSGs), and supernova explosions inject nucleosynthetic products of stellar interiors into the ISM, progressively increasing its metallicity. This constant recycling and associated enrichment drives the evolution of a galaxy's baryonic matter and changes its emission characteristics. To understand this recycling, we have to study the physical processes of the ISM, the formation of new stars, and the injection of mass by evolved stars, and their relationships on a galaxy-wide scale.

Infrared (IR) observations (Arendt et al. 1999, Sylvester et al. 1999; Groenewegen 1995) as well as isotopic analysis of stardust grains isolated from meteorites (Anders and Zinner 1993) have shown that a wide variety of sources contribute to the injection of dust in the interstellar medium. The relative contribution of these sources is not well known (Tielens et al. 2005). Galactic studies have shown that carbon-rich and oxygen-rich Asymptotic Giant Branch stars are important sources of carbonaceous and silicate grains (Speck et al. 1997, Sylvester et al. 1999). In addition, massive stars form dust – in the guise of RSGs as well as luminous blue variables – and contribute significantly (Jura & Kleinmann 1990). It is also often thought that massive stars form copious quantities of dust when they explode as supernovae (Dwek & Scalo 1980; Dwek 1988). Direct evidence for this is limited to a few supernovae – SN 1987A in the LMC the most notable example (Wooden et al. 1993; Fischera et al. 2002) – and sometimes controversial (Dunne et al. 2003; Krause et al. 2004). The recent discovery that high redshift galaxies contain copious amounts of dust despite the fact that low mass stars will not have had the time to evolve onto the AGB that early in the universe's history is generally taken as an indication that type II supernova are an important source of dust as well (Bertoldi et al. 2003; Schneider et al. 2004). However, supernovae also destroy dust as their ejecta drive strong shock waves through the interstellar medium. Dust grains are rapidly sputtered in shocks and, depending on material, calculated lifetimes of interstellar dust in the Milky Way are approximately 400 million year (Jones et al. 1994; 1996). This is much faster than the injection timescale of new dust by stars (1-2 billion years) and, yet, most of the heavy metals are in the form of dust grains (Sofia et al. 1994; Snow & Witt 1996). Hence, either we are missing a major stellar source of interstellar dust or the models grossly overestimate the destruction rate. Alternatively, dust is reformed efficiently in the ISM but in that case, the composition of interstellar dust can be expected to be different from that of the stellar sources and is likely to vary widely.

Among the nearby galaxies, the Large Magellanic Cloud (LMC) is the best astrophysical laboratory for studies of the lifecycle of the ISM, because its proximity ($\sim$50 kpc, Feast 1999) and its favorable viewing angle (35^o, van der Marel & Cioni 2001) permits studies of the resolved stellar populations and ISM clouds. All LMC features are at approximately the same distance from the Sun, and there is typically only one significant cloud along a given line of sight, so their relative masses and luminosities are directly measurable. The LMC also offers a rare glimpse into the physical processes in an environment with spatially varying sub-solar metallicity ($Z \approx 0.3 - 0.5 Z_\odot$, Westerlund 1997) that is similar to the mean

metallicity of the ISM during the epoch of peak star formation in the Universe ($z \approx 1.5$, Madau et al. 1996; Pei et al. 1999). The dust-to-gas mass ratio has real spatial variations and is ∼2–4 times lower than in the solar neighborhood (Gordon et al. 2003), resulting in substantially higher ambient UV fields than the solar neighborhood. The ISM gas that fuels star formation (Fukui et al. 1999; Staveley-Smith et al. 2003), the stellar components that trace the history of star formation (Harris & Zaritsky 1999; Van Dyk et al. 1999; Nikolaev & Weinberg 2000), and the dust (Schwering 1989; Egan et al. 2001, Meixner et al. 2006) have all been mapped at a variety of wavelengths. From the perspective of galaxy evolution, the LMC is uniquely suited to study how the agents of evolution, the ISM and stars, interact as a whole in a galaxy that has undergone tidal interactions with other galaxies, the MW and SMC (Zaritsky & Harris 2004; Bekki & Chiba 2005).

We have used *Spitzer* to survey the LMC ($7^o \times 7^o$) using IRAC and MIPS in our cycle 2 program entitled *Spitzer Survey of the Large Magellanic Cloud: Surveying the Agents of a Galaxy's Evolution* (SAGE, PI: Margaret Meixner, PID 20203; http://sage.stsci.edu; Meixner et al. 2006). The full IRAC and MIPS-24 point source catalogs have been made available to the scientific community in December 2006, containing about 4 million sources, and further data release are planned. The SAGE survey detects all the important points in the life cycle of dust; emission from the diffuse ISM with column densities $> 1.2 \times 10^{21}$ H cm^{-2}, newly formed stars with masses $> 3\,M_\odot$ and evolved stars with mass loss rates $> 1 \times 10^{-8}\,M_\odot$ yr^{-1}, promising to leave a major Spitzer legacy.

Previous infrared surveys of the LMC were hampered by sensitivity and hence limited to only the brightest sources. The resulting census was therefore skewed to the tip of the AGB and some bright supergiants (e.g. Egan et al. 2001; Cioni et al. 2000). Spitzer with its sensitive arrays has allowed for the first time a full census of all objects brighter than $\sim 15^{\rm th}$ magnitude in IRAC [8.0] in the LMC, as produced in the SAGE survey.

1.2 Spectroscopic follow up to SAGE (SAGE-Spec)

The wealth of information from SAGE will not reach its full potential without infrared spectroscopy. In particular, a quantitative analysis of these SAGE data requires knowledge of the detailed spectral appearance to distinguish between sources of similar IRAC and MIPS colors, and properly interpret the stellar population in the LMC, as it is reflected by the SAGE catalog. **We propose a comprehensive spectroscopy program of dust in the LMC with the goal to determine the composition, origin and evolution, and observational characteristics of interstellar dust and its role in this nearby galaxy** (See Fig. 3-left for the targets' locations, Fig. 2, 3, 4 for their properties).

This spectroscopy program is a logical and necessary extension of the SAGE IRAC and MIPS mapping study of the LMC, and we will utilize MIPS in SED mode and IRS to meet these specific objectives:

- To follow the life cycle of dust and molecular gas in a wide variety of environments and metallicities of relevance to the lifecycle of matter, ranging from stardust production sites (AGB stars, red supergiants, post–AGB–objects, planetary nebulae), to the interstellar medium (atomic and molecular clouds) to star forming regions (HII regions, young stellar objects).

- To relate the SAGE photometry to dust characteristics for different types of objects. The derived color classification will be coupled back to the entire SAGE catalog, thus

further boosting the combined SAGE and SAGE-Spec legacy value. This color classification scheme will also be of great value for the analysis and interpretation of observations of more distant galaxies.

1.3 Following the life cycle of dust and gas with IRS and MIPS SED

Methods - Infrared spectroscopic studies provide a unique tool for probing the composition, origin and evolution of interstellar dust. Whereas photometric measurements provide basic information on the global physical properties of dust grains, the individual constituents of the grain population can only be studied through their characteristic spectral signatures, in the infrared often due to thermal emission, but occasionally – particularly in the case of ices – in absorption (See Fig. 1, left panel). The dominant solid state components – silicates, oxides, ices, carbides, sulphides – exhibit resonances in the mid- and far-infrared that act as an identifying fingerprint allowing identification, and determination of properties like grain shape, grain size, total column density and temperature (e.g. Molster & Kemper 2005, Gibb et al. 2004). Specifically, the MIPS SED wavelength range gives access to additional water ice features (Hoogzaad et al. 2002).

In addition, polycyclic aromatic hydrocarbons (PAHs) dominate the mid-IR spectra of the ISM through their characteristic vibrational signature. PAHs do not radiate thermal emission like the larger dust grains discussed above. Rather, they require excitation by UV irradiation, before cascading back to lower energy levels produces the commonly observed infrared emission bands in the near- and mid-infrared (e.g. van Diedenhoven et al. 2004, Van Kerckhoven et al. 2000). Therefore, PAHs are global tracers of the UV flux and hence of young and massive star distributions. In that sense, PAH emission is often used as a global tracer of star formation.

Finally, several molecular and atomic emission lines may be detected in the infrared regime (e.g. Fig. 1-right) particularly in regions with a strong radiation field or in shocked regions (e.g. Bernard-Salas et al. 2004, Smith et al. 2004), providing diagnostic tools for the physical conditions in these regions. Towards low mass loss rate AGB stars, the warm molecular gas can be observed in absorption (e.g. Matsuura et al. 2006, Speck et al. 2006) unveiling the conditions of dust formation.

In our studies, we will probe all representative stages of the life cycle of dust using SAGE-selected targets. Specifically:

Evolved stars - For the dust forming evolved stars, we will address the following questions: How are the properties of the progenitor star (e.g. mass and metallicity) related to the spectra of the AGB, post-AGB/PPNe and PNe? Is the dust condensation sequence in the LMC comparable to the Galactic sequence, or do we find further evidence for the enhanced carbonaceous dust production? In order to answer these questions we will observe low-mass loss rate AGB stars, and combine these data with IRS observations of extreme AGB stars already extensively covered in the ROC (Fig. 2). We will also obtain spectroscopy of the subsequent post-AGB and PNe phases to follow the evolution of the dust as the stellar wind material is dispersed into the ISM. We focus on field stars, as well as a sample of objects from clusters with known metallicities and ages, providing a unique handle on the effect of these parameters on the newly formed dust characteristics. In particular, we are interested in the transition from oxygen to carbon star which seems to occur for a wider range of stars than at Galactic metallicities (Zijlstra et al. 2006).

Diffuse interstellar medium - We will obtain spatially integrated spectroscopy of molecular and atomic clouds using both MIPS SED and the low resolution IRS modules. We will determine the properties of dust and PAHs in these clouds and address how the properties of the dust evolve after being deposited into the ISM. In irradiated regions, such as HII regions, the surface brightness will be high enough to investigate spatial variations in the properties of dust and PAHs, and correlate this with the interstellar radiation field measured through PAH feature strengths and atomic line ratios (e.g. Fig. 4, left panel).

Star formation and young stars - Besides HII regions illuminated by massive young stars, the SAGE survey and the proposed SAGE-Spec follow-up are at the LMC distance well suited to detect the more heavily embedded phases of star formation, the Young Stellar Objects (YSOs; Fig. 2). In this phase, the infrared spectra are dominated by thermal emission from the dust in the circumstellar envelope, and using radiative transfer models, the physical properties and chemical composition of the dust shell can in principle be determined. While the SAGE photometry constrains the YSO parameter space (Robitaille et al. 2006), the proposed IRS and MIPS SED observations are a prerequisite for fully understanding the physical characteristics of the YSO population. In addition, the spectra will reveal whether the dust composition and grain properties in YSOs reflect those in the interstellar medium, or whether additional processing has occurred. It will also be possible to follow the condensation of volatile components (ices) that do not exist in the diffuse ISM. Finally, SAGE-Spec will provide definitive spectral identification of the YSOs which inhabit areas of color-magnitude space that are also covered by other types of objects (PNe, post-AGB stars, background galaxies; Fig. 2).

Serendipitous sources - We expect the serendipitous discovery of background galaxies in our survey, as they may exhibit the same infrared colors as our intended targets. In context of the SAGE and SAGE-Spec programs, these will be important for classification purposes, but we recognize that they are also of interest in their own right. One of us (Varoujan Gorjian) will analyze the spectra of these objects and place them in their specific context.

1.4 The classification of sources in the SAGE survey of the LMC

The only infrared classification scheme of point sources in the LMC (Egan et al. 2001) is shown to have its limitations. It is based upon color and luminosity templates for the Milky Way (Cohen 1993), and only includes the brightest infrared sources as it is limited by the MSX capabilities ($7.5^{\rm th}$ magnitude at $\sim$8 μm).

We plan to use the SAGE-Spec survey of IRS and MIPS SED observations, alongside already existing observations of LMC sources in the Spitzer archive, to create a more appropriate LMC based color-classification scheme. The data of the already existing observations, covering a distinctly different area in the color-magnitude diagram than the observations proposed here (Fig. 2), will be reduced and analyzed through the same pipeline as the rest of the sources, yielding a coherent spectral catalog. The spectral classifications will be coupled back to the SAGE catalog, with the goal to provide spectral typing of the sources in the catalog as a synergetic component of the SAGE and SAGE-Spec programs.

2 Technical Plan

2.1 Point sources - IRS observations

In order to explore the full life cycle of dust in the LMC and to completely classify the sources in the SAGE photometric catalogs, we propose IRS and MIPS SED spectroscopy of a large, but carefully selected sample of sources that cover the range in luminosities and color found in the SAGE data (Figs. 2,3 and 4). Previous studies (e.g. Buchanan et al. 2006; Zijlstra et al. 2006) have already targeted point sources in the LMC with the IRS. These sources – predominantly (extreme) AGB stars – concentrate in the brightest part of the [8.0] vs. [8.0]-[24] color-magnitude diagram (Fig. 2) in an area hereafter referred to as the *ROC exclusion region*. The proposed point sources (Fig. 3, Tab. 1) are selected with the aim to complete the coverage of color-magnitude space, while, at the same time, ensuring that all important classes in the lifecycle of dust are sufficiently covered.

AGB star candidates (18 O-rich, 18 C-rich) were selected from a larger pool of about 6000 evolved stars that have measured excess emission in the 8 or 24 μm wavelengths due to dust emission. We identify carbon star candidates ($\sim -0.8 < [8.0]-[24] < 3.8$; $\sim 11 > [8.0] > 5$) and oxygen-rich AGB star candidates ($\sim 0 < [8.0]-[24] < 4$; $\sim 11 > [8.0] > 5$), partially overlapping in color-magnitude space. We have sampled the color-magnitude space corresponding to a range in mass-loss rates and main-sequence masses in the objects in a mostly uniform way, selecting slightly more objects in the color-magnitude areas with higher source density.

Cluster AGB stars (36) have been selected from clusters with known ages and metallicities, yielding targets of a much better pedigree than field stars. The clusters have been divided in bins of old ($\log t > 9$), medium ($8 < \log t < 9$), and young age ($\log t < 8$), and in bins of high ([Fe/H] > -0.5), medium ($-0.75 <$ [Fe/H] < -0.5) and low metallicity ([Fe/H] < -0.75). From each bin at least 3 stars were selected, although for some bins a large range of observed [8.0]-[24] colors necessitated a bettter sampling of up to $\sim$10 stars.

Post-AGB stars (7) are rare; the total number in the LMC is expected to be around 20–150, an estimate based on scaling the number for the Milky Way (100–300 post-AGB stars; Szczerba et al. 2001) down with the size of the LMC. To ensure incorporation of this type of targets in the sample, we have specifically selected 7 of the 17 post-AGB candidates identified by Alcock et al. (1998) and Wood & Cohen (2001).

Planetary Nebulae (12) were not selected based on their IR colors, but were instead drawn from the lists of LMC PNe assembled by Leisy et al. (1997) and Reid & Parker (2006), representing an adequate sampling of the diversity in the following observables: **1)** Electron density and temperature based on HST imaging. **2)** Morphology, including bipolar, arcuate, or possessing associated filamentary or diffuse nebulosity, as well as PNe whose structure changes radically with IRAC wavelength. **3)** IR color, with colors $0 < [4.5]-[8.0] < 5.5$.

Young stellar object candidates (88) occupy the region of color-magnitude space with $[24] > 7.7$ in Fig. 2, alongside planetary nebulae, and evolved stars such as extreme AGBs and post-AGBs, in unknown ratios. At the faint end of the distribution, a contribution from background galaxies is present. We will measure some sources in the latter region to explore the defining characteristics of YSOs vs. galaxies. In addition we selected point sources from the SAGE catalog uniformly in the relatively large region above and to the right of the LL observation limit (Fig. 2-left), with a lower source density in the region at $[8.0] > 10.5$.

CMD space fillers (14) In order to fully cover the observed SAGE colors we sample several underrepresented regions, such as $[3.6]-[8.0] > 5$ and the region bordered by $[8.0] > 9$ and $J > 13.3$ (Fig. 2). Given their unknown nature, these *CMD fillers*, may, in spite of their name, turn out to be very exciting objects!

The resulting source list is limited by the boundaries of the *ROC exclusion region*. The only exception is the inclusion of cluster stars from the *ROC exclusion region*, as the known age and metallicity are a definite advantage towards the analysis. We arrive at a target list containing 193 sources, all of which will be observed in SL, while 124 of these will also be observed in LL. The coverage of color-magnitude space of this selection is shown in Fig. 2.

A S/N of 60 in SL is required to analyze the spectral contribution from the dust in our spectra, as demonstrated by the data with a range of S/N (12, 60, 120) shown in Fig. 1-middle. The majority of our spectra will exhibit both a stellar and a dust contribution, and in some cases (early AGB stars, YSOs), we expect to observe dust features with a contrast as low as 15%. A S/N of 60 will give us a effective S/N of 4 in the dust alone, sufficient for a spectral classification. In LL, the S/N requirements are less stringent because the spectra that show dust at these wavelengths generally have more predominant features. A S/N of 30 will enable us to distinguish the MgS sulfide in carbon-rich environments and the crystalline features possible in AGB stars and YSOs. The observations will be carried out in staring mode, which we found to be about 30% more time efficient than cluster mode, due to the vast range of flux levels in our sample. The peak up targets are place holders, and will be replaced by suitable 2MASS targets if the proposal gets approved, adding up to 30s to an AOR, equivalent to 1.6 hrs of telescope time.

2.2 Point sources - MIPS SED observations

The SAGE-Spec IRS point source list combined with the IRS observations in the Spitzer archive, where matched with the SAGE archive for MIPS 70 μm detections. A minimum flux level of 100 mJy at 70 μm is required to obtain a S/N of $\sim$3 for 20×10s integrations. This will be sufficient to determine the slope of the SED, and characterize the dust in terms of grain size and temperature. We have selected 48 point sources to be observed with MIPS SED, covering a range in $[24]-[70]$ colors and F_{70} flux levels ranging from 100 mJy to several Jy (Fig. 4-right). The MIPS SED observations of the brighter sources will also allow us to discern strong spectral features, particularly atomic emission lines (as in Fig. 4-right) and emission due to ices (Hoogzaad et al. 2002), in addition to the principal goals of measuring grain size and temperature. The exact integration times are determined based on the 70 μm flux, and the slope of the SED. We apply a $+1'$ chop distance.

2.3 Extended sources

The interstellar medium environments in our sample – HII regions and atomic and molecular clouds – will be observed using the IRS spectral mapping mode and MIPS SED mode. We will apply two different observing strategies to reflect brightnesses of the two target types. For both strategies, dedicated off-source observations are needed to remove the time dependent IRS detector hit pixels and zodiacal light background – following the SSC's recommended observation strategy. While the exact AORs vary from source to source, depending on brightness, geometry and size, each observation – on-source and off-source – will consist of at least 4 measurements of each point on the sky to give a good amount of redundancy to

account for hot pixels, cosmic rays, etc.

The HII regions have been selected on size and the density as measured in Hα emission (Kennicutt & Hodge 1986). The source list covers a range in sizes from $1'$ to $16'$, while the density range spans about 2 orders of magnitude. HII regions cover only part of IRAC/MIPS color-color space in the LMC (green dots in Fig. 3-right). Areas with significantly lower surface brightness (red and blue dots) have different colors, and we selected 10 additional clouds from these (Fig. 3, Tab. 3).

IRS - The goal of the atomic and molecular cloud observations is to obtain S/N = 10 spectra spatially integrated over a $1' \times 1'$ region, allowing us to measure the strength ratios of the specific spectral features such as PAHs, and atomic emission lines such as [SIV]/[SIII], [NeIII]/[NeII] and [SIII] 18μm/[SIII] 34μm (Fig. 4-left). In addition, both SL and LL observations are required to get a good understanding of the dust emission. This translates to a S/N of 0.3 and 0.85 per pixel for the SL and LL spectra. Exposure times of 2×14s (SL) and 2×30s (LL) correspond to S/N values of 0.66/0.82 (SL2/SL1) and 0.71/0.52 (LL2/LL1), assuming an average source brightness of 1 (SL) and 0.3 (LL) MJy/sr. The best practices recommends a redundancy of 4 and so our exposure times (per pixel) will be 4×14s and 4×30s and we will map a $1' \times 1'$ region of each of the 8 diffuse targets.

In HII regions the spatial distribution of the aromatic and atomic line emission probe variations in the physical conditions, and we aim to achieve a S/N of 10 for a minimum of 8 spatial bins across the diameter of the source. On average, the HII regions are 5 and 10 MJy/sr (with a wide variation) at 8 and 24 microns, corresponding to a S/N of 1.5/2.2 (SL2/SL1) and 9.3/6.7 (LL2/LL1) per pixel assuming the shortest possible exposure times of 2×6s – or 4×6s when taking redundancy into account. This means we will have to integrate over $9'' \times 9''$ regions (5x5 pixels) at the shortest wavelengths to achieve our desired S/N of 10. All selected HII regions are at least $60''$, and we will map them in strips of $1' \times$ diameter of HII region. The mapping is done such that the SL slit is stepped in the cross-slit direction by the diameter and by 2 in the slit direction. The LL slit is stepped in the cross-slit direction by $1'$ and in the slit direction by the diameter of the HII region, thus obtaining a $1'$ wide slit in both LL and SL. The maximum length of an IRS AOR is 6 hours which limits the total length of the strip to $5.4'$. The largest HII regions in our sample will therefore not be mapped to their full diameter.

MIPS SED - For the HII regions, the MIPS SED observations roughly coincide with the peak of the SED and may also pick up strong [OI] 63 μm and [OIII] 88 μm lines (both were detected in 30 Dor observations taken during the Spitzer IOC, see Fig. 1, right panel). For the atomic and molecular regions the MIPS SED observations will constrain dust temperatures, and, in particular, the very small grain emisison properties.

To either determine the shape of the continuum or to detect the presence of emission lines, a S/N of 5 is required. Following best practices we will map each with 1/2 slit offsets in both slit dimensions ($9''$ cross-slit and $1.25'$ along-slit), with minimum exposure time. The achieved 5-sigma detection limit is 0.24, 0.58, and 1.29 Jy for 60, 75, and 90 μm, respectively. The average 70 μm surface brightness is 100 MJy/sr for the HII regions and 20 MJy/sr for the diffuse regions, translating to a $18'' \times 18''$ spatial element of 0.76 Jy and 0.15 Jy respectively. Thus, we will achieve the necessary S/N per spatial bin in the HII regions, while for the diffuse regions, the objective is the global SED over a $1' \times 1'$ region. The minimum exposure time, which yields a S/N of $\sim$5 for the average flux level in our targets (0.15 Jy), suffices.

3 Legacy Data Products Plan

The SAGE-Spec team organization is modeled after the successful SAGE project with three main data centers which will handle the data processing and four science teams which will lead the science efforts and provide the ultimate test of the data quality before delivery. At the University of Arizona, Karl Gordon, a member of the MIPS instrument team, will lead the processing of the MIPS SED point and extended source (MP&ME) data and the IRS extended sources maps (IRSE), using his extensive experience with IRS spectral maps in SINGS. At Cornell University, Greg Sloan, a member of the IRS instrument team, will lead the processing of the IRS point source (IRSP) data which are all taken in staring mode, for which he has developed efficient pipe-line processing. At Space Telescope Science Institute (STScI), Margaret Meixner, who is PI of SAGE and led the SAGE database effort, will lead the SAGE-Spec database (DB) effort, a natural extension to the current SAGE database. At NASA/Ames, Xander Tielens, an international authority on infrared spectroscopy and PI of the SAGE-Spec team, will provide the broad oversight to the SAGE-Spec science effort. At the University of Manchester, Ciska Markwick-Kemper, an expert in astromineralogy and evolved stars, will coordinate the evolved star (ES) science effort. At the University of Virginia, Remy Indebetouw, an expert on star formation studies with Spitzer, will coordinate the star formation (SF) science effort. At the Spitzer Science Center, William Reach, an international authority on the ISM, will coordinate the ISM science effort. At CfA-Harvard, Massimo Marengo, will coordinate the source classification (SC) based on the combined SAGE-Spec and SAGE results. All the other team members will be involved in these efforts as noted by the list of acronyms listed adjacent to their name on the cover page.

The SAGE-Spec team plans to deliver the following data products to Spitzer Science Center (SSC) for the community. **Reduced spectra** will be produced in the form of ascii tables, fits files and post-script plots; for both point sources and extended sources. In case of the spectral maps performed on extended sources, the data will be spatially averaged into one spectrum. **Spectral data cubes** will be produced for spectral maps with sufficient surface brightness (HII regions) using CUBISM, a now publicly available tool produced by J.D. Smith as part of the SINGS legacy program. From those data cubes, **maps in selected features or spectral lines** will be provided for extended regions with sufficient flux in the intended features. These data products will be collected at the SAGE-Spec database at STScI for use by the SAGE-Spec team and as a staging area for delivery to the SSC.

In addition, the SAGE-Spec team plans to deliver two enhanced science products based on these IRS and MIPS-SED spectra and the SAGE database photometry: 1) a set of **point source templates and extended source templates** that can be used for source classification in other galaxies and 2) a fully **classified SAGE point source catalog**. The proposed IRS and MIPS-SED sources and the existing IRS sources in the ROC will be used as templates for source classification of the whole SAGE catalog. These SAGE sources have photometry from the SAGE database which has U band through 160 μm photometry for each source detected by SAGE, down to the sensitivity limits of the IRAC, MIPS, 2MASS and MCPS (Zaritsky et al. 2004) catalogs. The SAGE sources will be classified using a statistical technique based on the weighted k-Nearest Neighbor method (k-NN, Fix & Hodge 1951, Hechenbichler & Schliep, 2004), adapted for the spectro-photometric classification of astronomical sources (Marengo et al. 2006). This method of classification requires a large template sample to characterize the Spitzer colors of the LMC sources and remove the degeneracy of sources of different classes with similar broad band colors and magnitudes.

4 Figures and Tables

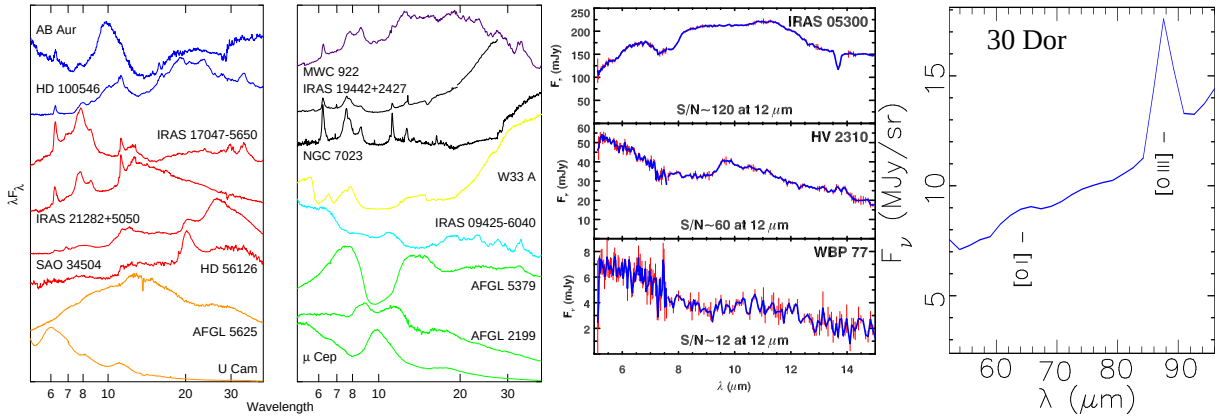

Figure 1: **Left:** Variety of spectral features in the IRS range observed in galactic sources using ISO-SWS spectroscopy. **Middle:** IRS-SL pectra (blue lines) with different S/N (red bars). The top spectrum has a S/N of $\sim$ 120 providing an excellent possibility to distinguish dust and molecular components. The bottom spectrum with a S/N of $\sim$ 12, shows a dust feature around 10-12 μm, although the details of the composition cannot be extracted. The middle spectrum at S/N $\sim$60 offers a good compromise between integrate time and data quality. **Right:** MIPS SED observations of the 30 Dor region in the LMC, taken during IOC. Indicated are the detections of the 88 μm [OIII] and 63 μm [OI] transitions.

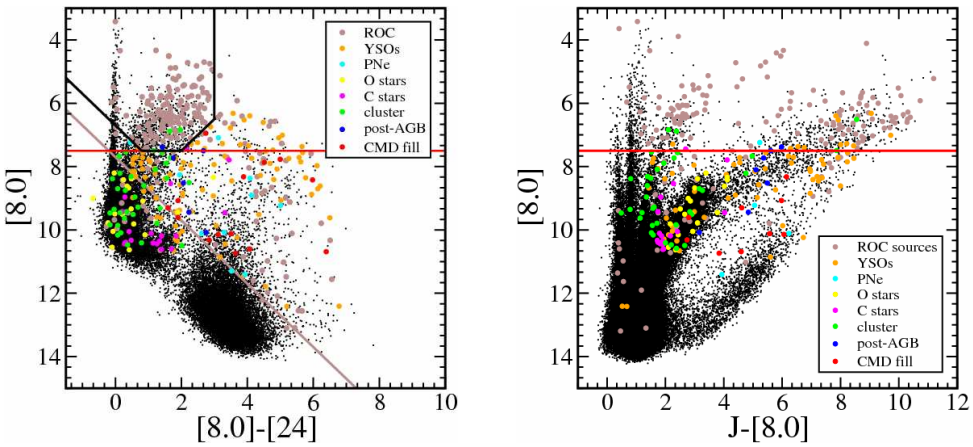

Figure 2: **Left:** [8] vs. [8]-[24] color-magnitude diagram. The black dots represent all sources in the SAGE catalog, the grey solid circles are the sources that are currently listed in the ROC as observed with IRS, mostly above the MSX A band detection limit (red line) and in the *ROC exclusion region* (black lines). The IRS point source selection is shown with colored solid circles. **Right:** [8] vs. J-[8] color-magnitude diagram with the same color coding.

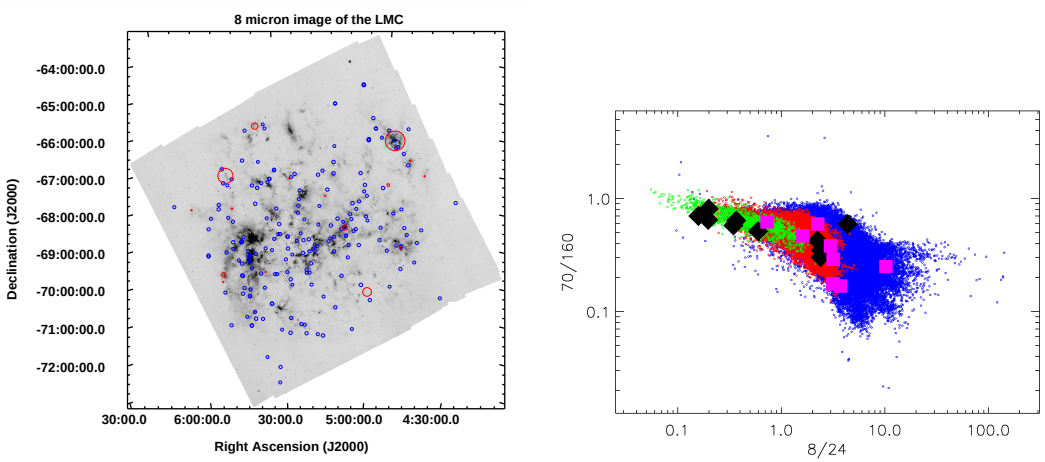

Figure 3: **Left:** Spatial distribution of the selected targets superposed on the SAGE IRAC-8.0 μm map of the LMC. The IRS point sources are indicated with blue circles, and the extended regions are indicated with red circles, where the size of the circles reflects the extent of the planned observations. **Right:** IRAC/MIPS color-color diagram of extended emission covering the entire LMC. The green, red and blue points indicate 160 μm surface brightnesses greater than 200, 50 and 10 MJy/sr respectively. The black diamonds represent the selected HII regions, and the purple squares are for the atomic and molecular clouds.

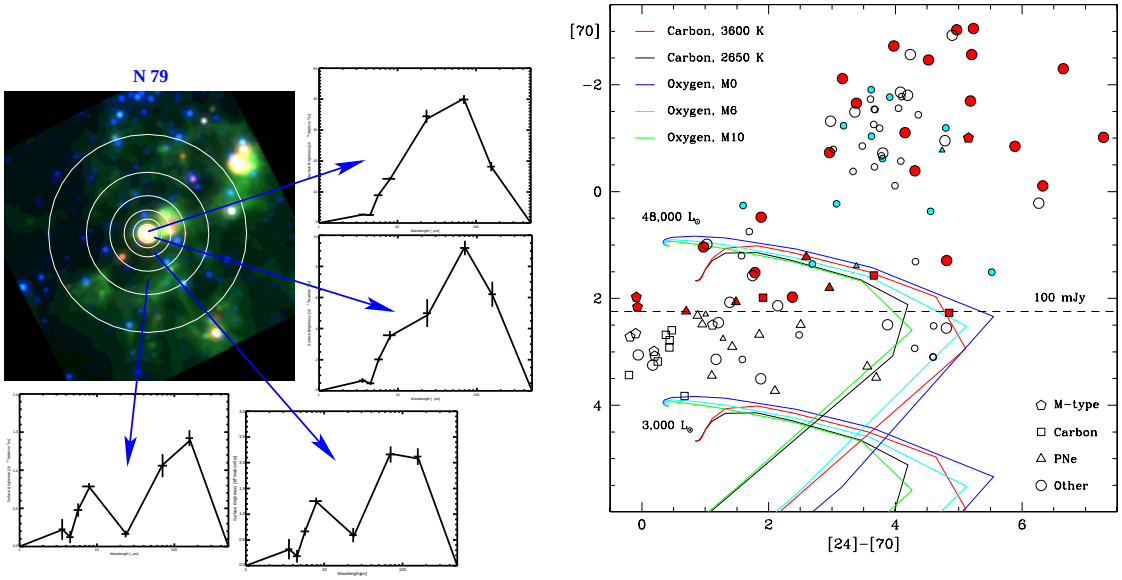

Figure 4: **Left:** Example of the prominent variations observed by SAGE around HII regions in the LMC. The image shows the N79 region in a composite of IRAC4.5, IRAC8 and MIPS160 . The graphs highlight the variations of the average SED as a function of distance. The distance scale probed here is typical for the size we propose to observe with IRS/MIPS SED. Without these proposed observations the predominant dust temperature (MIPS-SED) and the relative contributions from hot small grains or PAHs at 8 μm (IRS) are ill constrained. **Right:** [70] vs. [24]-[70] color-magnitude diagram. Small symbols indicate objects in SAGE-Spec, large symbols objects with IRS observations in the archive; in color our selection for MIPS SED follow-up. Indicated are calculated evolutionary tracks of different types of objects. The dashed line indicates our 100 mJy observation limit.

5 References

Alcock et al. 1998, ApJ 115, 1921
Anders & Zinner 1993, Meteoritics 28, 490
Arendt et al. 1999, ApJ 521, 234
Bekki & Chiba 2005, MNRAS 356, 680
Bernard-Salas et al. 2004, ApJS 154, 271
Bertoldi et al. 2003, A&A 406, L55
Buchanan et al. 2006, AJ 132, 1890
Cohen 1993, AJ 105, 1860
Cioni et al. 2000, A&A 359, 601
Dunne et al. 2003, Nature 424, 285
Dwek 1988, ApJ 329, 814
Dwek & Scalo 1980, ApJ 239, 193
Egan et al. 2001, AJ 122, 1844
Feast 1999, PASP 111, 775
Fischera et al. 2002, A&A 395, 189
Fukui et al. 1999, PASJ 51, 745
Gibb et al. 2004, ApJS 151, 35
Gordon et al. 2003, ApJ 594, 279
Groenewegen 1995, A&A 293, 463
Harris & Zaritsky 1999, AJ 117, 2831
Hoogzaad et al. 2002, A&A 389, 547
Jones et al. 1994, ApJ 433, 797
Jones et al. 1996, ApJ 469, 740
Jura & Kleinmann 1990, ApJS 73, 769
Kennicutt & Hodge 1986, ApJ 306, 130
Krause et al. 2004, Nature 432, 596
Leisy et al. 1997, A&AS 121, 407
Madau et al. 1996, MNRAS 283, 1388
Matsuura et al. 2006, MNRAS 371, 415
Molster & Kemper 2005, Space Sci. Rev. 199, 3
Nikolaev & Weinberg 2000, ApJ 542, 804
Pei et al. 1999, ApJ 522, 604
Reid & Parker 2006, MNRAS 373, 521
Robitaille et al. 2006, ApJS 167, 256
Schneider et al. 2004, MNRAS 351, 1379
Smith et al. 2004, ApJS 154, 199
Schwering 1989, A&AS 79, 105
Snow & Witt 1996, ApJL 468, 65
Sofia et al. 1994, ApJ 430, 650
Speck et al. 1997, MNRAS 288, 431
Speck et al. 2006, ApJ 650, 892
Staveley-Smith et al. 2003, MNRAS 339, 87
Sylvester et al. 1999, A&A 352, 587
Szczerba et al. 2001, in *Post-AGB objects as a phase of stellar evolution*, eds. R. Szczerba & S.K. Górny, p. 13
Tielens et al. 2005, in *Chondrites and the protoplanetary disk*, ASP Conf. Series 341, p. 605-631
van der Marel & Cioni 2001, AJ 122, 1807
van Diedenhoven et al. 2004, ApJ 611, 928
Van Dyk et al. 1999, in *New views of the Magellanic Clouds*, IAU Symp. 190, p. 363
Van Kerckhoven et al. 2000, A&A 357, 1013
Westerlund 1997, *The Magellanic Clouds*
Wood & Cohen 2001, in *Post-AGB objects as a phase of stellar evolution*, eds. R. Szczerba & S.K. Górny, p. 71
Wooden et al. 1993, ApJS 88, 477
Zaritsky & Harris 2004, ApJ 604, 167
Zijlstra et al. 2006, MNRAS 370, 1961

6 Brief Resume/Bibliography

Resumes and research interests of key investigators

Xander Tielens (PI) has published extensively on the physics and chemistry of interstellar dust and gas over the last twenty years. In particular, using ground-based, airborne, and space-based observatories, his studies have focussed on the infrared spectroscopy of interstellar and circumstellar dust. He is the NASA project scientist for SOFIA and the (European) project scientist for HIFI, the heterodyne instrument on Herschel.

Ciska Markwick-Kemper (TC) was one of the inaugural recipients of the Spitzer Fellowship, and now at the University of Manchester. She studies the formation and evolution of dust in galactic and extragalactic environments, and is an expert on astromineralogy.

Karl Gordon has worked on dust in the Milky Way and other galaxies in the local universe. As a member of the MIPS Instrument Team and the SINGS and SAGE Legacy teams he has extensive experience with Spitzer data analysis.

Greg Sloan specializes in infrared spectroscopy of dust and molecules. As a member of the IRS GTO team he has a strong involvement in the calibration of IRS spectra and development of analysis tools.

Margaret Meixner has 66 refereed publications with an emphasis on infrared diagnostics of dust and gas in circumstellar environments and PDRs. Meixner is PI of the SAGE legacy program; the SAGE homepage is at http://sage.stsci.edu.

Summary bibliography of relevant publications by team members

Blum, R.D.; Mould, J.R.; **Olsen, K.A.**; et al. 2006 *Spitzer SAGE survey of the Large Magellanic Cloud II: Evolved Stars and Infrared Color Magnitude Diagrams* AJ 132, 2034

Galiano, F.; **Madden, S.C.**; Jones, A.P.; Wilson, C. & **Bernard, J.-Ph.** 2004, *ISM properties in low-metallicity environments: III. The dust spectral energy distribution of II Zw 40, He 2-10 and NGC 1140*, A&A 434, 867

Gordon, K.D.; Misselt, K.A., Witt, A.N. & Clayton, G.C. 2001, *The DIRTY model. I. Monte Carlo radiative transfer through dust*, ApJ 531, 269

Gorjian, V.; Werner, M.W.; Mould, J.R.; **Gordon, K.D.** et al. 2004, *Infrared imaging of the Large Magellanic Cloud star-forming region Henize 206*, ApJS 154, 275

Kemper, F.; Vriend, W.J. & **Tielens, A.G.G.M.** 2004, *The absence of crystalline silicates in the diffuse interstellar medium*, ApJ 609, 826

Meixner, M.; **Gordon, K.**; **Indebetouw, R.**; et al., 2006 *Spitzer Survey of the Large Magellanic Cloud, Surveying the Agents of a Galaxys evolution (SAGE): I. Overview and initial results*, AJ 132, 2268

Reach, W.T.; Boulanger, F.; Contursi A. & Lequeux, J. 2000, *Detection of mid-infrared solid-state emission features from the Small Magellanic Cloud*, A&A 361, 895

Robitaille, T.P.; **Whitney, B.A.**; **Indebetouw, R.**; Wood, K., & Denzmore, P. 2006, *Interpreting Spectral Energy Distributions from Young Stellar Objects. I. A Grid of 200,000 YSO Model SEDs* ApJS, 167, 256

Sloan, G.C.; Kraemer, K.E.; **Matsuura, M.** et al. 2006, *Mid-infrared spectroscopy of carbon stars in the Small Magellanic Cloud*, ApJ 645, 1118

Ueta, T. & **Meixner, M.** 2003, *2-Dust: A dust radiative transfer code*, ApJ 586, 1338

Zijlstra, A.A.; **Matsuura, M.**; Wood, P.R.; **Sloan, G.C.**; **Lagadec, E.** et al. 2006, *A Spitzer mid-infrared spectral survey of mass-losing carbon stars in the Large Magellanic Cloud*, MNRAS 370, 1961

7 Observation Summary Table

Designation	Type	RA (J2000)	Dec (J2000)	$F_{5.8}$ (mJy)	$F_{8.0}$ (mJy)	F_{12} (mJy)	F_{24} (mJy)	mode	int. time (s)
14976396	Clst.	69.33818	-70.579085	6.1	4.3	3.5	1	SL	8x60
J043727.60-675435.0	CMD	69.365004	-67.909735	0.7	5.5	6.9	11.1	SL/LL	3x60/3x120
J044627.10-684747.0	YSO	71.612926	-68.796399	44.2	37.2	30.1	9	SL/LL	2x14/4x120
J044717.51-690930.2	YSO	71.822965	-69.158402	14.8	45.8	264	918.6	SL/LL	3x6/3x6
J044718.64-694220.5	YSO	71.827671	-69.705702	34	21.4	17.7	6.6	SL/LL	3x14/6x120
J045040.54-685818.8	YSO	72.668918	-68.971899	42	34.7	27.6	6.3	SL/LL	2x14/8x120
J045128.59-695550.0	CMD	72.869161	-69.930557	12.1	14.8	13.5	9.7	SL/LL	2x60/3x120
J045140.56-684734.8	CMD	72.919011	-68.793002	44.1	105.1	116.1	149.2	SL/LL	3x6/3x6
J045200.37-691805.4	YSO	73.001557	-69.301515	4.3	9	108.5	407.1	SL/LL	3x6/3x6
J045201.16-692007.5	YSO	73.004854	-69.335418	31.4	64.6	197.3	595.6	SL/LL	3x6/3x6
8932838	Clst.	73.135508	-67.049838	21	19.9	15.7	3	SL	4x14
J045309.37-681711.0	C	73.289079	-68.28639	6.8	4.2	3.3	0.6	SL	10x60
J045328.70-660334.5	O	73.369598	-66.059585	29.6	27.1	21.3	3.9	SL	3x14
J045330.10-691749.3	YSO	73.375442	-69.297038	10.7	40.9	354.4	1295	SL/LL	3x6/3x6
J045405.75-664506.9	YSO	73.523963	-66.751932	97.3	154.8	278.2	648.4	SL/LL	3x6/3x6
8997405	Clst.	73.595228	-70.449196	47.1	28	21.7	2.9	SL	3x14
J045526.69-682508.5	YSO	73.861239	-68.41904	10.9	22.7	213	784	SL/LL	3x6/3x6
J045550.58-663434.6	YSO	73.960778	-66.576299	55.8	91.8	317.8	995.8	SL/LL	3x6/3x6
J045622.59-663656.8	YSO	74.094139	-66.615785	12.1	28.8	187.3	662.7	SL/LL	3x6/3x6
J045623.22-692748.8	YSO	74.096783	-69.463571	none	10.7	10.5	9.9	SL/LL	2x60/3x120
J045659.83-662425.9	CMD	74.249301	-66.40721	8.9	29.6	52.3	120.4	SL/LL	3x6/3x6
J045842.46-660835.5	YSO	74.676934	-66.143202	7.7	17.8	134.8	485.7	SL/LL	3x6/3x6
J045855.02-691118.5	O	74.729257	-69.188474	11.9	10.1	7.8	1.1	SL	2x60
RP1805	PN	74.730625	-68.843389	1.6	3.9	2.9	none	SL	12x60
9199676	Clst.	74.781438	-67.743255	18.4	10.3	8	1	SL	2x60
J050032.60-662112.9	YSO	75.135869	-66.353593	1.9	4.2	5.7	10.2	SL/LL	4x60/3x120
RP1631	PN	75.143583	-70.866694	29.4	31.9	29.2	21.4	SL/LL	2x14/3x30
9366357	Clst.	75.589478	-66.110602	134.7	116.2	107.3	80.7	SL/LL	3x6/3x6
9368847	Clst.	75.600801	-66.110329	18.7	25	24.3	22.1	SL/LL	2x14/3x30
A7	PAGB	75.770833	-68.673611	15.2	24.8	23.3	18.7	SL/LL	2x14/4x30
J050316.59-654945.0	O	75.819149	-65.829194	32	33	25.6	3.6	SL	2x14
J050336.92-683338.4	O	75.903846	-68.560688	29.9	28	22.2	5	SL	2x14
J050342.58-675919.0	C	75.927432	-67.988618	6.9	4.7	3.7	0.8	SL	8x60
J050353.37-702747.5	O	75.972392	-70.463213	23.7	21.5	17	3.5	SL	4x14
9468241	Clst.	76.031018	-66.445276	18	10.4	8.2	1.4	SL	2x60
9468522	Clst.	76.03225	-66.418285	12.7	9.9	7.9	1.8	SL	2x60
9471856	Clst.	76.046069	-66.437979	26.9	16.4	13.1	3.2	SL	2x60
J050428.91-674123.9	YSO	76.120468	-67.689974	36.4	41.5	40.7	38.4	SL/LL	3x6/3x14
RP1878	PN	76.142542	-67.872694	4.3	5.8	6.2	7.2	SL/LL	3x60/3x120
J050517.07-692156.9	CMD	76.321151	-69.365829	2	3.6	7.1	17.5	SL/LL	3x60/4x30
J050555.64-672209.7	YSO	76.481872	-67.369382	20	16.2	12.9	3	SL	2x60
J050558.23-680923.5	CMD	76.492664	-68.156535	1.7	3.2	5	10.5	SL/LL	4x60/3x120
J050607.54-714148.2	O	76.531426	-71.696735	31.1	22.5	17.8	3.5	SL	3x14
9595092	Clst.	76.552423	-64.927143	6	3.7	2.8	none	SL	12x60
9601703	Clst.	76.579063	-64.936218	5.5	4.1	3.2	0.7	SL	10x60
9602919	Clst.	76.583834	-64.916307	21.4	20.9	16.3	2.5	SL	4x14
J050629.58-685534.7	O	76.623283	-68.926324	7.1	7.8	6	0.7	SL	3x60
J050639.15-682209.1	YSO	76.663141	-68.369213	0.8	0.7	2.8	9.3	SL/LL	12x60/4x120

Tab. 1 Point source list for IRS staring mode observations.

Designation	Type	RA (J2000)	Dec (J2000)	$F_{5.8}$ (mJy)	$F_{8.0}$ (mJy)	F_{12} (mJy)	F_{24} (mJy)	mode	int. time (s)
9654433	Clst.	76.789162	-68.980379	66.4	54.2	42.4	6.8	SL/LL	3x6/6x120
J050752.91-681246.5	YSO	76.970467	-68.21294	32.1	29.8	23.9	6	SL/LL	2x14/8x120
J050759.37-683925.7	YSO	76.997375	-68.657152	12.2	17.4	16.3	12.9	SL/LL	4x14/2x120
J050826.35-683115.1	YSO	77.109813	-68.520866	48	42.7	34	7.9	SL/LL	2x14/6x120
J050830.53-692237.3	O	77.127219	-69.377054	12.5	29.1	34.5	50.5	SL/LL	2x14/2x14
J050836.44-694315.7	O	77.151854	-69.721038	7.1	6	4.8	1	SL	6x60
9803313	Clst.	77.360781	-69.115604	9.7	5.8	4.5	0.8	SL	6x60
9806647	Clst.	77.373175	-69.130621	3.2	4	3.7	2.9	SL	8x60
J050949.10-685230.5	YSO	77.454617	-68.875157	46.1	80	82.5	90.2	SL/LL	3x6/3x6
J051024.09-701406.4	YSO	77.600379	-70.235135	85.5	143.9	360.7	1011	SL/LL	3x6/3x6
9870880	Clst.	77.618073	-68.742057	60	63.5	52.9	21.1	SL/LL	3x6/3x30
J051059.08-685613.8	C	77.746189	-68.937168	31.2	24.3	21.4	12.9	SL/LL	3x14/2x120
J051209.03-710649.6	YSO	78.037639	-71.113802	42.7	67.4	73.6	92.2	SL/LL	3x6/3x6
J051213.54-683922.7	YSO	78.05644	-68.656327	7.4	6.1	5.7	4.5	SL	4x60
J051301.77-693351.0	CMD	78.257399	-69.564182	5.6	45.1	115.6	327.4	SL/LL	3x6/3x6
J051306.37-690946.3	YSO	78.276576	-69.162885	78.6	69.2	55.5	14.6	SL/LL	3x6/6x30
J051339.93-663852.3	C	78.416401	-66.647885	6.4	4.6	3.9	1.8	SL	8x60
10085506	Clst.	78.41822	-65.464626	18.9	11.9	10.1	4.7	SL	2x60
10086623	Clst.	78.42248	-65.474507	12	7.2	5.6	0.9	SL	4x60
J051342.61-672410.0	YSO	78.427574	-67.402782	0.8	0.7	10.6	40.3	SL/LL	2x60/2x14
J051348.36-670527.1	YSO	78.451526	-67.090868	1.1	1.7	3	6.9	SL/LL	12x60/6x120
J051412.33-685057.9	C	78.551398	-68.849435	6.1	4.2	3.6	1.6	SL	8x60
A11	PAGB	78.575417	-69.209722	42.8	51.1	45.6	29.3	SL/LL	3x60/2x30
J051453.12-691723.5	C	78.721363	-69.289874	4.8	10.5	14.2	25.2	SL/LL	2x60/3x30
J051526.48-675126.6	C	78.86034	-67.857402	6.8	4.4	3.5	0.7	SL	8x60
J051612.39-704930.2	C	79.051662	-70.82506	5.9	4.3	3.6	1.4	SL	8x60
J051618.70-715358.8	YSO	79.077919	-71.899677	25.7	62.1	164.5	471.6	SL/LL	3x6/3x6
J051654.06-672005.0	YSO	79.225267	-67.334749	33.9	53.9	72.8	129.7	SL/LL	3x6/3x6
J051747.19-681842.5	YSO	79.44664	-68.311824	3.3	3.4	3.1	2.1	SL	10x60
J051803.28-684950.6	YSO	79.513679	-68.830738	39.1	31	24.6	5.7	SL/LL	2x14/8x120
J051807.94-715153.5	O	79.533093	-71.864871	10.7	7.5	6	1.4	SL	3x60
J051811.10-672648.4	YSO	79.546284	-67.446782	42.6	27.9	24.1	12.7	SL/LL	2x14/2x120
10424315	Clst.	79.636077	-69.423743	11.5	10.7	8.5	1.7	SL	2x60
J051908.47-692314.2	O	79.785327	-69.387288	16.8	15.8	12.1	1	SL	2x60
J051910.47-693345.3	YSO	79.793656	-69.562607	18.5	19.4	15.7	4.9	SL	4x14
J051944.81-692959.4	C	79.936742	-69.499854	5.1	3.6	3.2	2	SL	10x60
J052014.23-702930.8	C	80.059304	-70.49191	5	3.6	3	1.5	SL	10x60
J052023.96-695423.2	YSO	80.09984	-69.906463	18.5	27.3	85.1	258.7	SL/LL	3x6/3x6
J052051.81-693407.6	C	80.215886	-69.568805	6.4	5.3	4.8	3.3	SL	6x60
J052052.42-700935.5	YSO	80.218424	-70.159877	24.9	73	140.2	341.8	SL/LL	3x6/3x6
J052101.64-691417.4	YSO	80.256864	-69.238176	10.2	11.2	10.3	7.6	SL/LL	2x60/6x120
W3	PAGB	80.452083	-70.165278	59.1	70.8	60.5	29.8	SL/LL	3x6/2x30
A2	PAGB	80.455417	-70.076389	7.2	10.6	10.3	9.3	SL/LL	2x60/4x120
J052206.92-715017.6	CMD	80.528841	-71.838238	5.9	9.1	8.3	5.9	SL/LL	2x60/8x120
J052222.95-684101.0	YSO	80.595655	-68.68363	12.3	26.3	38.8	76.3	SL/LL	3x6/3x6
J052241.94-691526.0	YSO	80.674753	-69.257249	64.6	60.2	48.8	14.7	SL/LL	3x6/6x30
J052245.11-713610.1	YSO	80.687981	-71.60281	44.5	75.6	128.3	286.5	SL/LL	3x6/3x6
J052254.95-693651.9	YSO	80.72896	-69.614424	5	4.6	4.2	2.9	SL	6x60

Tab. 1 continued

Designation	Type	RA (J2000)	Dec (J2000)	$F_{5.8}$ (mJy)	$F_{8.0}$ (mJy)	F_{12} (mJy)	F_{24} (mJy)	mode	int. time (s)
LMC55	PN	80.88	-69.067889	2.3	6	7.9	13.9	SL/LL	2x60/2x120
J052335.55-675235.6	YSO	80.89815	-67.876574	25.3	52	287.5	993.9	SL/LL	3x6/3x6
J052351.11-680712.1	YSO	80.962996	-68.120052	43.6	60	362.5	1270	SL/LL	3x6/3x6
J052353.93-713443.7	YSO	80.974709	-71.57883	93.4	122.1	177.3	343	SL/LL	3x6/3x6
J052405.31-681802.5	YSO	81.022163	-68.300704	41.2	34.7	27.7	6.8	SL/LL	2x14/6x120
J052413.34-682958.7	YSO	81.055613	-68.499654	118.7	174.4	342	844.9	SL/LL	3x6/3x6
J052445.39-691605.2	YSO	81.189137	-69.268135	68.7	51.8	42	12.8	SL/LL	3x6/2x120
J052457.86-672458.2	CMD	81.241103	-67.416188	12.1	12	10.6	6.2	SL/LL	2x60/8x120
J052601.22-673011.8	YSO	81.505084	-67.503294	20.7	37	125.9	392.6	SL/LL	3x6/3x6
J052620.09-693902.2	YSO	81.583732	-69.650624	7	5.5	5	3.6	SL	4x60
RP589	PN	81.656583	-70.485278	3.1	3.7	2.8	none	SL	12x60
J052707.07-702001.9	YSO	81.779485	-70.333865	9.7	10.7	9.6	6.6	SL/LL	2x60/6x120
J052723.13-712426.2	YSO	81.8464	-71.407299	4.6	15	53.5	169.2	SL/LL	3x6/3x6
11064809	Clst.	81.898485	-69.148985	90.3	157	117.8	none	SL	3x6
J052738.56-692843.9	YSO	81.91069	-69.478871	73.1	50.6	45.8	31.5	SL/LL	3x6/2x30
11069607	Clst.	81.915134	-69.150385	97.1	60.8	47.9	9.2	SL/LL	3x6/4x120
J052747.58-714852.7	YSO	81.948277	-71.814646	32.8	37.5	34.9	27	SL/LL	2x14/2x30
J052805.87-700753.5	YSO	82.024462	-70.131532	35.6	31.7	27.9	16.6	SL/LL	2x14/6x30
J052825.78-694647.2	O	82.107423	-69.779802	14.5	11.6	9.2	2.1	SL	2x60
J052954.71-690415.6	YSO	82.477971	-69.071013	64.4	45.1	37.2	13.6	SL/LL	3x60/2x120
J053004.57-684728.7	YSO	82.519062	-68.79133	43.6	29.2	23.8	7.6	SL/LL	2x14/6x120
J053027.51-690358.1	C	82.614663	-69.066141	8.6	6	4.8	1	SL	6x60
J053044.10-714300.4	CMD	82.683768	-71.716791	9.5	49.2	176.4	558	SL/LL	3x6/3x6
J053044.99-682129.1	YSO	82.68748	-68.358107	56	49.4	39.4	9.2	SL/LL	3x6/4x120
11284036	Clst.	82.695042	-67.282563	15.2	8.9	7	1.3	SL	3x60
11285736	Clst.	82.70171	-67.279415	36.4	22.9	18.6	5.7	SL/LL	3x14/8x120
11290099	Clst.	82.717791	-67.292913	42.4	28.3	24.6	13.4	SL/LL	2x14/2x120
J053128.42-701027.2	YSO	82.868452	-70.174226	33.7	44.8	41.8	32.7	SL/LL	3x6/3x14
A9	PAGB	82.962083	-69.196111	33.3	63.2	68.3	83.7	SL/LL	3x6/3x6
J053158.92-724435.7	O	82.995522	-72.743263	7.3	5.5	4.5	1.4	SL	6x60
11373508	Clst.	83.027998	-70.173579	9.4	5.4	4.3	0.7	SL	6x60
11386744	Clst.	83.077748	-67.52943	48.9	29.8	23.7	5.2	SL	2x14
11387548	Clst.	83.080592	-67.52238	119.5	111.6	98.2	57.9	SL/LL	3x6/3x6
J053226.51-731006.6	O	83.110466	-73.168524	11.3	9.9	7.8	1.3	SL	2x60
RP775	PN	83.185	-69.501528	36.7	93.6	116.3	184.4	SL/LL	3x6/3x6
J053253.35-660727.6	YSO	83.222309	-66.124354	0.7	1.2	3.2	9.2	SL/LL	10x60/4x120
J053254.99-673647.2	O	83.229139	-67.613113	17.4	14.6	11.9	3.6	SL	2x60
J053318.59-660040.2	YSO	83.327489	-66.011182	49.2	48.6	40	14.2	SL/LL	3x6/6x30
11478888	Clst.	83.430375	-70.989202	20.9	12.3	9.9	2.6	SL	2x60
11479642	Clst.	83.433345	-70.983863	12.3	7.7	6.4	2.8	SL	3x60
J053346.96-683644.1	YSO	83.445669	-68.612263	22.3	77.7	102	175.1	SL/LL	3x6/3x6
RP793	PN	83.672917	-69.441778	86.4	81.5	64.5	13.7	SL/LL	3x6/2x120
J053444.17-673750.1	YSO	83.684061	-67.630602	15.2	20.3	21.7	26.2	SL/LL	3x14/2x30
J053518.91-670219.5	YSO	83.828818	-67.038763	94.4	76.5	75.4	72.3	SL/LL	3x6/3x6
J053548.05-703146.5	C	83.950238	-70.529607	7.4	5.3	4.5	2.2	SL	6x60
J053602.34-674517.2	YSO	84.00978	-67.754782	none	5.1	8.1	17.3	SL/LL	2x60/6x30
J053634.78-722658.5	CMD	84.144944	-72.449601	5.6	5.7	8.3	16	SL/LL	2x60/6x30
J053642.40-700746.6	YSO	84.176687	-70.129627	17.2	42.2	50.4	75.2	SL/LL	3x6/3x6

Tab. 1 continued

Designation	Type	RA (J2000)	Dec (J2000)	$F_{5.8}$ (mJy)	$F_{8.0}$ (mJy)	F_{12} (mJy)	F_{24} (mJy)	mode	int. time (s)
J053655.61-681124.5	YSO	84.231741	-68.190154	5.7	4.8	4.4	3.1	SL	6x60
RP493	PN	84.29225	-71.387194	1.3	1.9	2.8	5.5	SL	12x60
J053730.57-674041.6	YSO	84.377385	-67.678241	7.2	9.9	22.8	61.6	SL/LL	2x14/3x6
J053754.78-693435.6	YSO	84.478283	-69.576563	24.8	43.7	126	372.8	SL/LL	3x6/3x6
J053823.59-660900.1	YSO	84.598301	-66.150041	15.6	15.9	13.4	5.6	SL	2x60
J053929.95-695755.8	YSO	84.874814	-69.965516	47.8	44.1	35.6	10.3	SL/LL	2x14/3x120
A6	PAGB	84.887917	-71.365278	3.2	5.9	6.5	8.4	SL/LL	3x60/4x120
J053942.46-711044.3	YSO	84.926923	-71.178999	9.4	17	20.1	29.6	SL/LL	3x14/2x30
J053945.38-665809.5	YSO	84.939103	-66.969316	7.8	7.1	6.4	4.3	SL	3x60
J053949.17-693747.1	CMD	84.95488	-69.629774	1	3.3	36.7	136.9	SL/LL	3x6/3x6
J053959.48-693730.2	YSO	84.997864	-69.62508	47.3	99	372	1191	SL/LL	3x6/3x6
A10	PAGB	85.002083	-69.703889	31.1	36.3	27.2	none	SL	2x14
J054000.66-694713.3	YSO	85.002781	-69.787049	35.8	71.3	424.2	1483	SL/LL	3x6/3x6
J054014.77-692849.1	YSO	85.061578	-69.480329	97.5	187.6	283.1	569.4	SL/LL	3x6/3x6
RP85	PN	85.139875	-70.544528	5.7	17.5	35	87.4	SL/LL	2x14/3x6
J054059.29-704402.6	YSO	85.24706	-70.734057	17.9	30.8	77.1	216	SL/LL	3x6/3x6
J054101.95-704311.0	C	85.258127	-70.719732	69.3	66.5	63.7	55.5	SL/LL	3x6/2x14
J054114.54-713236.0	O	85.310589	-71.543335	8.5	10.5	9.5	6.8	SL/LL	2x60/6x120
J054120.72-690443.7	YSO	85.336365	-69.078816	45.6	126.2	145.9	205	SL/LL	3x6/3x6
J054157.39-691218.2	YSO	85.489133	-69.205074	51.4	37.6	31.4	12.7	SL/LL	2x14/2x120
11951476	Clst.	85.489204	-69.205049	50.4	36.7	30.7	12.7	SL/LL	2x14/2x120
11957234	Clst.	85.516184	-69.218732	52.9	44	38.1	20.5	SL/LL	3x6/3x30
11959703	Clst.	85.528124	-69.208682	61.7	59.8	51.1	25	SL/LL	3x6/3x30
11962536	Clst.	85.541465	-69.22469	59	51.3	45.2	27	SL/LL	3x6/2x30
J054230.52-694857.2	C	85.627172	-69.815913	23.4	16.4	12.9	2.4	SL	2x60
SMP88	PN	85.63875	-70.49	1.3	1.8	3.1	7.3	SL/LL	10x60/6x120
J054233.73-711727.8	YSO	85.640557	-71.291076	none	50.4	218.5	722.7	SL/LL	3x6/3x6
SMP89	PN	85.654167	-70.158639	8.2	28.8	56.2	138.6	SL/LL	3x6/3x6
J054254.35-700807.4	YSO	85.726463	-70.135391	13.7	8.9	7.6	3.6	SL	2x60
J054310.85-672727.9	C	85.795249	-67.457774	18	48.4	69.1	131.1	SL/LL	3x6/3x6
J054314.09-703835.1	C	85.808742	-70.643088	17.7	10.7	8.4	1.5	SL	2x60
J054328.74-694243.7	YSO	85.869791	-69.71216	9.2	9.1	7.7	3.3	SL	2x60
J054405.98-683753.6	YSO	86.02492	-68.631563	45.1	32.6	27.3	11.4	SL/LL	2x14/3x120
J054437.85-673657.6	YSO	86.157728	-67.616027	59.1	52.3	41.9	10.7	SL/LL	3x6/3x120
J054440.11-691149.0	CMD	86.167162	-69.196965	2.9	4.7	5.4	7.3	SL/LL	4x60/6x120
J054450.20-692304.3	YSO	86.209175	-69.384529	9	20.9	184.5	675.5	SL/LL	3x6/3x6
J054524.22-683041.4	YSO	86.350941	-68.511519	1.2	2.9	3.7	6	SL/LL	8x60/8x120
J054544.80-670928.2	YSO	86.436675	-67.157838	32.3	50.7	102.7	259	SL/LL	3x6/3x6
J054546.30-673239.3	YSO	86.442934	-67.544271	13.8	18.3	17.1	13.5	SL/LL	4x14/2x120
SMP92	PN	86.769583	-69.45925	4.5	13	46.4	146.5	SL/LL	3x6/3x6
J054745.76-680734.1	YSO	86.940676	-68.126149	17.8	23.5	21.7	16.3	SL/LL	3x14/6x30
J054757.33-681457.0	O	86.988878	-68.249174	5.6	3.8	3	0.4	SL	12x60
12246875	Clst.	87.070053	-71.477593	40	32.8	25.6	4.2	SL	2x14
J054900.00-703322.6	CMD	87.250005	-70.556282	3.4	27	208.9	754.4	SL/LL	3x6/3x6
J055036.65-682852.3	O	87.652735	-68.48121	5.1	3.5	2.8	0.6	SL	12x60
J055143.26-684543.0	YSO	87.930258	-68.761955	6.2	7.1	8.7	13.5	SL/LL	2x60/2x120
12399911	Clst.	88.212725	-69.477654	10	7.3	5.7	0.7	SL	4x60
12400566	Clst.	88.218764	-69.509874	19.5	11.5	8.9	1.3	SL	2x60
J060053.60-680038.8	C	90.223351	-68.010804	8.6	5.7	4.7	1.8	SL	6x60

Tab. 1 continued

name	RA (J2000)	Dec (J2000)	notes	F_{70} (mJy)	int. time (s)
MIPS SED observations of point sources with IRS data in the ROC:					
IRAS04553-6825	73.793661	-68.341651	RSG/OH maser	1770	8x10
IRAS05298-6957	82.352212	-69.921086	M-AGB/OH maser	108.3	20x10
IRAS05329-6708	83.214015	-67.114385	M-AGB/OH maser	128	20x10
WOH-G457	85.049793	-70.154362	M-AGB or RSG?	1992	7x10
MSX-LMC45	77.665162	-68.601355	C	126.8	20x10
MSX-LMC349	79.362191	-68.916299	C	186.5	20x10
IRAS05291-6700	82.281638	-66.970868	C	97.63	20x10
IRAS04515-6710	72.907574	-67.08806	PN	100.4	20x10
LHA120-N97	76.216559	-68.652646	PN	150.6	20x10
SMP-LMC-28	76.990104	-68.863138	PN	256	20x10
IRAS05257-7135	81.229485	-71.548924	PN	118	20x10
IRAS05047-6644	76.1959	-66.675077	YSO?	12860	3x10
MSX-LMC222	78.424945	-69.590754	YSO?	13150	3x10
IRAS05216-6753	80.37368	-67.851846	YSO?	16720	3x10
IRAS05325-6629	83.133108	-66.454232	YSO?	8389	3x10
IRAS05328-6827	83.160778	-68.422879	YSO	1551	12x10
30Dor-17	84.367051	-69.146602	YSO?	3633	3x10
Dor-IRS166	84.762351	-69.134651	YSO	6578	3x10
LI-LMC1501E	84.924414	-69.769977	YSO	24350	3x10
IRAS04530-6916	73.190414	-69.197057	emission line	5546.7	3x10
HD268835	74.196155	-69.840227	B8Iae	509	20x10
HV269006	75.53083	-71.336946	LBV?	1750	9x10
SNR0525-66.1	81.512913	-66.088104	SNR	872.9	20x10
IRAS05280-6910	81.916901	-69.134613	OH/IR	7007	3x10
HV2671	83.453833	-70.223224	R CrB	128.3	20x10
HD37974	84.107692	-69.382151	Be	304.4	20x10
LHA120-N89	73.777197	-69.285699	?	7651	3x10
MSX-LMC577	81.627637	-67.67686	?	2184	6x10
MSX-LMC783	83.230985	-69.340721	?	241	20x10
MSX-LMC741	83.857639	-71.332396	?	195.8	20x10
LHA120-N158B	84.685562	-69.410625	?	9735	3x10
UFO1	85.049281	-70.167829	?	2014	7x10
30Dor?	85.179924	-70.186196	?	1132	20x10
MSX-LMC1794	85.183352	-69.431807	?	3771	7x10
MSX-LMC956	85.205279	-70.170435	?	1727	9x10
MIPS SED observations of IRS point source targets in SAGE-Spec					
IRAS04537-6922	73.375442	-69.297038	YS/WR?	622.6	20x10
IRAS04557-6639	73.960778	-66.576299	YSO	4034	3x10
IRAS04562-6641	74.094139	-66.615785	YSO	2056	6x10
J052222.95-684101.0	80.595655	-68.683630	YSO?	563.3	20x10
HS270-IR1	80.974709	-71.578830	YSO/postAGB?	641.1	20x10
HD36402	81.505084	-67.503294	YSO/WR?	1396	14x10
IRAS05281-7126	81.846400	-71.407299	YSO?	227.1	20x10
N160	84.997864	-69.625080	YSO	2464	5x10
LHA120-N159S	85.002781	-69.787049	YSO	4582	3x10
IRAS05458-6710	86.436675	-67.157838	YSO?	2370	5x10
J043727.60-675435.0	69.365004	-67.909735	CMD	197.3	20x10
RP775	83.185000	-69.501528	PN	1612.5	10x10
RP85	85.139875	-70.544528	PN	219	20x10

Tab. 2 Planned MIPS SED observations for a selection of point sources with IRS observations planned in this SAGE-Spec proposal, or with IRS data already present in the ROC.

RA (J2000)	Dec (J2000)	size	$F_{8.0}$ (MJy/sr)	F_{24} (MJy/sr)	F_{70} (MJy/sr)	F_{160} (MJy/sr)
mol/atomic clouds - IRS: 1x14/1x30s; MIPS SED: 1x3s int. time per pointing						
82.958333	-68.508333	$1.0' \times 1.0'$	2.97	1.84	47.74	102.69
86.000000	-68.291667	$1.0' \times 1.0'$	1.47	0.49	14.71	38.69
79.112917	-68.030000	$1.0' \times 1.0'$	1.05	0.33	7.40	25.63
71.866667	-67.295833	$1.0' \times 1.0'$	0.87	0.23	3.31	19.75
89.000000	-68.170000	$1.0' \times 1.0'$	1.12	0.36	6.60	37.69
87.320000	-70.260000	$1.0' \times 1.0'$	0.78	0.08	5.16	20.63
83.800000	-70.050000	$1.0' \times 1.0'$	1.43	0.64	23.50	39.60
81.591667	-67.537500	$1.0' \times 1.0'$	1.82	2.50	46.76	75.64
82.833333	-68.500000	$1.0' \times 1.0'$	5	3.4	85.7	166.2
83.125000	-66.483333	$1.0' \times 1.0'$	4.6	9.5	88.2	96.6
HII regions - IRS: 1x6/1x6s; MIPS SED: 1x3s int. time per pointing						
73.02629852	-66.92420197	$1.0'$	16.54	84.09	346.75	536.22
73.04959869	-69.34529877	$2.3'$	7.79	21.23	163.57	256.61
74.20870209	-66.41390228	$16.0'$	14.74	93.18	431.24	617.70
74.42169952	-67.64830017	$2.1'$	0.91	0.38	9.18	30.46
75.42169952	-70.64689636	$7.2'$	0.70	0.16	2.31	3.90
77.48329926	-68.90090179	$4.6'$	20.94	105.25	563.70	697.07
81.26789856	-71.46309662	$0.5'$	0.99	0.45	10.33	24.39
83.87960052	-66.04409790	$5.4'$	1.58	2.65	33.61	65.57
86.22460175	-67.34839630	$12.7'$	1.05	0.44	12.60	36.35
87.21829987	-70.06430054	$3.9'$	3.80	11.02	112.18	194.58

Tab. 3 Planned observations of extended regions, with IRS mapping and MIPS SED.

Mode	Type	Category	AOR time (hrs)
IRS	point sources	Cluster stars	16.8
		CMD fillers	10.0
		YSO candidates	47.8
		C-rich AGB candidates	11.5
		O-rich AGB candidates	8.2
		Planetary Nebulae	9.2
		post-AGB candidates	3.3
		peak-up correction	1.6
IRS	point sources	total	108.4
MIPS SED	point sources	O-rich stars	3.1
		C-rich stars	3.1
		Planetary Nebulae	5.7
		YSO candidates	8.4
		other objects	10.9
MIPS SED	point sources	total	31.2
IRS	extended emission	mol/atomic clouds	23.6
IRS		HII regions	40.6
MIPS SED		mol/atomic clouds	7.9
MIPS SED		HII regions	12.7
	extended emission	total	84.8

Tab. 3 AOR time overview.

8 Status of Existing Spitzer Programs

Co-I **K. Gordon** is the TC of the MIPS ERO program 717 to study M81, for which the data is published (Gordon et al. 2004, ApJS, 154, 215). He is also the TC of the MIPS GTO programs 60 and 30244 to study the HII regions in M101, and MIPS GTO programs 99 and 30203 to study M31. The PID 99 and PID 60 data have been obtained, and the first results are published (Gordon et al. 2006, ApJL 638, 87; Marleau et al. 2006, ApJ 646, 929). The data for PID 30203 and 30244 will be obtained this spring and summer. He is also the PI of the GO-2 program 20146. The final observations for this program have recently been taken and all the data has been reduced. Analysis of the full dataset is ongoing.

Co-I **S. Hony** is PI of GO-1 program 3345, for which the data have been obtained and GO-3 program 30737, for which the data are being collected.

Co-I **R. Indebetouw** is PI of PID 249; a publication is expected to be submitted this spring. He is also PI of a program for spectroscopy of 30Dor - the initial data reduction is complete, and the refinement of artifacts is ongoing.

Co-I **M. Marengo** is PI of PID 3441; for which all data is obtained and a paper is in preparation. He is also PI of PID 30754 and TC of PID 30335 and PID 30411. 50% of the data of these projects is obtained and preliminary results have been presented at conferences.

Co-I **F. Markwick-Kemper** is PI for GO-1 program 3591, and for DDT program 1094. The data for these programs have been obtained, and are currently being analyzed. For both programs, the first results are published (Markwick-Kemper et al. 2005, ApJL 628, 119; Speck et al. 2006 ApJ 650, 892), and four further papers are in advanced stages of preparation.

Co-I **M. Matsuura** is the TC for program 20357 (see Zijlstra).

Co-I **M. Meixner** is PI of the Cycle-2 Spitzer Legacy Program: Spitzer Survey of the Large Magellanic Cloud: Surveying the Agents of a Galaxy's Evolution (SAGE). The SAGE Epoch 1 IRAC point source catalog and archive, ∼4 million sources, and the SAGE Epoch 1 MIPS 24 μm point source catalog, ∼60,000 sources, were delivered to IRSA in December 2006 for the community, in less than a year from obtaining all of the data. Two papers have appeared in press (Meixner et al. 2006, AJ 132, 2268; Blum et al. 2006, AJ 132, 2034) and a further 12 are in preparation. SAGE results have been presented at several conferences, most recently at a SAGE special session at the January 2007 AAS meeting, where the team contributed 5 oral presentations, and 14 poster presentations.

Co-I **K. Olsen** is the PI of GO-2 program 20469. The data have been processed and are anticipated to be submitted for publication in March 2007.

Co-I **W. Reach** is PI of GO programs 3119, 3137 and 20039, DDT programs 256 and 274, and is the TC for GTO programs 210 and 30010. The results from programs 210, 3119, and part of 30010 are in two submitted papers. For program 3119 a paper is in preparation. Images from programs 20039 and 274 appeared in a press release, and are to appear in two papers. Program 256 on comet 9P/Tempel 1 is awaits its final observations.

Co-I **G. Sloan** is the TC for the IRS GTO MC_DUST program (PID 200), which has led to one paper, with two more in preparation. He is also the TC for a IRS Cycle 3 GO program to study evolves stars in nearby Local Group galaxies (PID 30333), and the PI on three small IRS Cycle 3 GTO programs (PIDs 30345, 30355, 30322). Observations for the Local Group program are underway; they are complete for the smaller programs.

Co-I **A. Speck** is PI of GO-2 program 20258, which observed 4 (post-)AGB stars using MIPS. These data have all been reduced and presented at several conferences. 2 peer re-

viewed publications have been forthcoming. Analysis continues but is hampered by poorly understood PSF.

Co-I **S. Van Dyk** is PI on DDT program 226 and 237, which are both finished and have resulted in two publications (Kotak et al. 2005, ApJL 628, 123; Kotak et al. 2006, ApJL 651, 117). He is also PI on GO programs 3641, 20574 and 20608. The observations are taken, and papers are in preparation.

Co-I **J.Th. van Loon** is PI of GO-2 program 20648 (IRAC and MIPS maps of ω Cen). The data have been taken and reduced, and a first paper is in preparation.

Co-I **B. Whitney** is PI of GO-3 Theory program 30467 to make a grid and fitter of star formation models publicly available. We have done this (http://caravan.astro.wisc.edu/protostars), submitted two publications that are in press, and are working on our next-generation grid of models.

Co-I **A. Zijlstra** is PI of GO program 20357: *Mass loss from AGB stars in local group galaxies.* Data has been obtained; analysis and modelling in progress. He is also PI of GO program 30333 GO: *Dust Production in Local Group Dwarf Galaxies.* Part of the observations have been obtained.

9 Proprietary Period Modification

No changes to the proprietary period of 0 months for legacy proposals are requested.

10 Justification of Duplicate Observations

There are no duplicate observations.

11 Justification of Targets of Opportunity

There are no ToO observations.

12 Justification of Scheduling Constraints

There are no constraints on this program.

13 Data Analysis Funding Distribution

Below, we provide an approximate distribution of the funds associated with the proposal. If our proposal gets accepted, and the funding level is known, we would like to re-assess the funding distribution.

- Meixner (STScI): 25%, subdivided as follows:
  - Salary Bernie Shiao, SAGE database programmer, 4 months
  - Graduate student, Sundar Srinivasan, 1 year
  - Salary Postdoc, Marta Sewilo, 1 year

  - Travel: 2 AAS and 1 international
  - Page charges for whole team: 230 pages, at $110/page

- Gordon (Arizona): 20%, subdivided as follows:

  - Salary data analyst, 6 months
  - Salary postdoc, 1 year
  - Travel: 2 people, 2 AAS meetings & 1 international each
  - Dedicated computer

- Sloan (Cornell): 20%, subdivided as follows:

  - Salary Greg Sloan, 3 months
  - Salary postdoc, 1 year
  - Travel: 4 visits to Manchester, UK + 2 AAS
  - Computer hardware: 1 dedicated system, 1 RAID storage system, computer for post-doc

- Tielens (NASA Ames): 10%, subdivided as follows:

  - Travel (2 AAS, 1 international)
  - Salary postdoc, 9 months

- Marengo (Harvard/CfA): 5% (4 months salary)
- Indebetouw (Virginia): 5% (6 months salary)
- Hora (Harvard/CfA): 4% (2 months salary)
- Cohen (Berkeley): 4% (2 months salary)
- Vijh (Toledo): 4% (6 months salary)
- Gorjian (NASA JPL): 1% (travel)
- Speck (Missouri): 1% (1 month summer salary)
- Van Dyk (IPAC/CalTech): 0.5% (travel)
- Reach (IPAC/CalTech): 0.5% (travel)

14 Financial Contact Information

For PI Xander Tielens:
Mr. Brett Vu
NASA Ames Research Center
MS 245-1
Moffett Field, CA 94035
email: Brett.Vu@nasa.gov
fax: +1 650-604-6779
Telephone: +1 650-604-0911

For co-I Martin Cohen:
Patricia A. Gates
Sponsored Projects' Office
University of California, Berkeley
2150 Shattuck Ave., Suite 313
Berkeley, CA 94704-5940
Phone: 510-642-8109; FAX: 510-642-8236
E-mail: pgates@berkeley.edu

For co-I K. Gordon
Sherry Esham, Director
University of Arizona
Sponsored Projects
PO Box 3308
Tucson AZ 85722-2208
520-626-6000 (phone)
520-626-4137 (fax)
sponsor@email.arizona.edu

For co-I Varoujan Gorjian:
Eloise S. Kennedy
email: eloise.kennedy@.jpl.nasa.gov
phone: +1 626 395-1810, Fax number: +1 626 397-7021
JPL, M/S: 100-22, 4800 Oak Grove Drive
Pasadena, CA 91109-8099

For co-Is Joe Hora and Massimo Marengo:
William Ford
Contract Administrator
Mail Stop 23
Smithsonian Astrophysical Observatory
60 Garden Street
Cambridge MA 02138-1516
617-495-7317
wford@cfa.harvard.edu

For co-I Remy Indebetouw:
Neal Grandy, Research Administrator
University of Virginia
PO Box 400772
Cabell Hall
Charlottesville, VA 22904
434-924-7130
nrg2p@virginia.edu

For co-I Margaret Meixner:
Lynn Kozloski
STScI
Contracts & Business
3700 San Martin Dr.
Baltimore, MD 21218
(410) 338-4355
kozloski@stsci.edu

For co-I William T. Reach and Schuyler Van Dyk:
Ms. Eloise Kennedy
IPAC/Caltech
Mailcode 100-22
Pasadena, CA 91125 USA
(626)395-1810 phone, (626)397-7021 fax
email: esk@ipac.caltech.edu

For co-I Greg Sloan:
Susan L. Jones
Cornell University
Sponsored Program Services
120 Day Hall
Ithaca, NY 14853
Phone 607-255-2945
Fax 607-255-5058
slj15@cornell.edu

For co-I Angela Speck:
Barb Savio
University of Missouri - Columbia
Office of Sponsored Program Administration
310 Jesse Hall
Columbia, MO 65211-1230
Phone: (573) 884-2794
Fax: (573) 884-4078
Email: savioba@missouri.edu

For co-I Uma Vijh:

Dorothy Spurlock
Director, Research and Sponsored Programs
Office of Research
The University of Toledo
2801 W. Bancroft St.
Toledo, OH 43606
419-530-2227
DSpurlo@UTNet.utoledo.edu